Julian D. Osorio
Center for Energy Conversion & Storage Systems,
National Renewable Energy Laboratory,
Golden, CO 80401
e-mail: julian.osorio@nrel.gov

Alejandro Rivera-Alvarez
Ingeniería Térmica Ltda.;
Fundación Ergon,
Medellín, Colombia
e-mail: ajrivera@ingenieriatermica.com

Obie I. Abakporo
Department of Mechanical Engineering,
FAMU-FSU College of Engineering,
Florida A&M University,
Tallahassee, FL 32310
e-mail: obiechina1.abakporo@famu.edu

Juan C. Ordonez
Department of Mechanical Engineering,
FAMU-FSU College of Engineering,
Energy and Sustainability
Center and Center for Advanced Power Systems,
Florida State University,
Tallahassee, FL 32310
e-mail: ordonez@caps.fsu.edu

Rob Hovsapian
Energy Systems Integration,
National Renewable Energy Laboratory,
Golden, CO 80401
e-mail: rob.hovsapian@nrel.gov

Thermodynamic Modeling of Heat Engines Including Heat Transfer and Compression–Expansion Irreversibilities

In this work, a thermodynamic model based on an endoreversible engine approach is developed to analyze the performance of heat engines operating under different thermodynamic cycles. The model considers finite heat transfer rate, variable heat source and sink temperatures, and irreversibilities associated with the expansion and compression. Expressions for the maximum power and efficiency at maximum power output are obtained as a function of hot and cold reservoir temperatures, the equivalent isentropic efficiency of compression and expansion components, and the effective conductance ratio between heat exchangers. In all cases, the Curzon–Ahlborn efficiency is retrieved at constant reservoir temperatures and neglected compression–expansion irreversibilities. The proposed model allows assessing the effect of isentropic efficiencies and heat exchanger design and operation characteristics for different thermodynamic cycles. [DOI: 10.1115/1.4050786]

Keywords: efficiency at maximum power, maximum power, heat engine, compression–expansion irreversibilities

1 Introduction

The development of efficient heat engines is a fundamental alternative to counteract the accelerated depletion of non-renewable energy sources during the last decades. The design and optimization of efficient heat engines require thermodynamic models that describe the engine performance, and how this performance is being impacted by the engine characteristics and operating factors. The maximum possible efficiency attained by heat engines operating between two energy reservoirs is set by the Carnot efficiency (η_C). It corresponds to the efficiency of heat engines operating in the reversible limit under quasi-static processes that results in zero power output [1]. In an effort to account for some of the main irreversibilities, models have been developed considering internally reversible engines where all irreversibilities occur during the energy exchange processes. From this approach, which considers the irreversibility of finite rate heat transfer, the efficiency at maximum power output (η_{CA}), also known as Curzon—Ahlborn efficiency, has been obtained [1–3]. This result was first presented by Chambadal [2] and Novikov [3]. Similar to η_C, η_{CA} is independent of the system characteristics, working fluid properties, or operation regimes, as it only depends on hot and cold reservoir temperatures. It was found that in the limit of low irreversibility, η_{CA} is bounded by $\eta_c/2$ and $\eta_c/(2-\eta_c)$ [4], i.e., $\eta_c/2 \le \eta_{CA} \le \eta_c/(2-\eta_c)$, and the bounds correspond to the extremes of the ratio of dissipation in the heat exchange processes. These studies have found that η_{CA} exhibits some degree of generality as it describes relatively well the efficiency of thermal cycles including Otto, Brayton, Stirling, and Ericsson cycles [5,6] and several real thermal plants [7–9].

In addition to the irreversibility of finite heat transfer rate, real thermal engines also present irreversibilities associated with the working fluid friction against turbine blades or friction between the piston and cylinder, pressure drop at heat exchangers, and heat leaks that decrease the efficiency and power output. Several models of efficiency at maximum power output that consider different sources of irreversibility such as finite compression ratio, irreversibilities inside the working fluid, heat leak loss, and fluid flow irreversibilities have been proposed [10–20]. Bejan [16] presented an analogy between the power conversion in a heat engine (thermal power conversion) and the extraction of power in a fluid flow driven by a pressure difference. It was shown in that work that, when the relationships between pressure difference and flow rates are linear, the energy conversion efficiency at maximum power is analogous to the Carnot efficiency. For nonlinear relationships between flow rate and pressure drops, the paper presents the conditions for operation at maximum power. In particular, for a turbine, the study looks at the effects of the pressure drops that occur in the ducting of the stream to the first expansion stage, the pressure drop across the turbine itself (characterized by an isentropic efficiency), and the discharge pressure drop. Maximum power can be obtained by selecting optimally the flow rate or the pressure drops associated with ducting the flow into and out of the turbine. Similar analyses are presented for compressors and pumps. Grazzini [17] presented the maximum available work and the maximum efficiency for an engine with heat transfer and internal irreversibilities and no heat leak. The engine cycle consisted of constant thermal-capacity heating and cooling processes together with polytropic and irreversible compression and expansion branches. The heat

Manuscript received December 4, 2020; final manuscript received March 26, 2021; published online June 11, 2021. Assoc. Editor: Cheng-Xian Lin.

source and heat sink were modeled as temperature changing fluid streams, whereas the internal irreversibility was given by an entropy-production amount dependent on the extent of the polytropic processes. In a different work, Ibrahim et al. [18] conducted a power output optimization of Carnot and closed Brayton cycles using Lagrange multipliers. In that work, the efficiency at maximum power output for both cycles was analyzed and compared under the same specific boundary conditions. Based on this analysis, the closed Brayton cycles can produce more power than the Carnot cycle. Also, in that work, a generic expression for the efficiency at maximum power output for both cycles, as a function of an entropy change parameter during heat addition and rejection, was developed. A finite-time optimization for an ideal Rankine cycle was proposed by Lee and Kim [19]. In that work, a general expression for the efficiency at maximum power output as a function of the reservoir, sink, and pinch-temperature difference of the heating and cooling fluids was obtained. In another study, Lee and Kim [20] considered a model of a heat engine consisting of two isothermal processes and two adiabatic processes. The adiabatic processes (expansion and compression) were treated as irreversible and the isothermal processes of heat addition and heat rejection were driven by fluids of finite capacity rates. By modeling the heat exchangers, their model captured the temperature variation of the hot and cold streams that drive the cycle. They maximized the power output, and corresponding efficiency, with respect to temperatures of the isothermal processes, and showed the dependence of power output on heat conductance, temperature levels, and internal irreversibility in the expansion/compression. They also showed that it is possible to maximize two times the power with respect to temperature levels and conductance allocation. In most of these studies, expressions for the efficiency at maximum power output smaller than η_{CA} have been obtained including parameters accounting for the additional source of irreversibility. As expected, η_{CA} is recovered from the efficiency expressions when the additional irreversibilities (other than the finite heat transfer rate) are neglected.

Besides the efficiency at maximum power output, several indicators such as maximum efficient power [8,21], maximum power density [22], ecological criterium [23], as well as methods including thermo-economic analysis [24], exergoeconomic analysis and optimization [25], entropy generation minimization [26], and ecological and exergetic performance optimization [27] have been developed to assess the performance of thermal engines and analyze the effect of system configuration, new designs, and operating parameters. For instance, the ecological criterium proposed by Angulo-Brown [23] allows the quantification of heat engines performance based on the trade-off between the power produced and the power loss in the heat engine as a result of the entropy generation. Different studies have performed analysis and optimization based on this criterion for diverse thermal cycles including Brayton, Stirling, and Ericsson [28–31]. The development of the generalized model capable of describing the behavior of any thermal cycle has been constantly pursued. Chen et al. [32] developed a model based on finite-time thermodynamics and ecological optimization to produce general expressions for the power, efficiency, and entropy generation rate of Diesel, Otto, Brayton, Atkinson, among other characteristic thermodynamic cycles. An exergoeconomic analysis and optimization were performed for a heat engine cycle consisting of two constant thermal-capacity heating, two constant thermal-capacity cooling, and two adiabatic branches [25]. The heat engine model in that work included heat transfer irreversibilities, as well as heat leakage, and internal irreversibilities due to compression and expansion. Importantly, in that study, the heat source and heat sink temperatures were considered constant, while the internal irreversibilities were treated through a coefficient greater than one relating the heat released by the engine under irreversible conditions to the heat released in the reversible case.

Besides the traditional derivation of the Curzon–Ahlborn efficiency, some alternative approaches have been used in the last years to get the same result based on different models [33], which contribute to highlight the features and limitations of the result. For example, Van den Broeck [34] obtained the result based on linear irreversible thermodynamics theory that does not use the explicit assumption of heat transfer processes or a reversible compartment. Also, another approach was used by Esposito et al [35], which is commonly referred to as low dissipation model.

In this work, a comprehensive model based on the endoreversible engine approach was developed to analyze the performance of several types of heat engines, including internal combustion engines, steam cycles, gas turbines, and organic Rankine cycles. The model considers finite heat transfer rate, variable heat source and sink temperature, and irreversibilities associated with the fluid friction losses, which are lumped into isentropic efficiencies of compression and expansion components. The model presented in this paper shares commonalities with models available in the literature addressing maximization of efficiency at maximum power output. Also, it presents similarities regarding the exploration of thermal conductance allocation, temperatures distribution, and the investigation of several sources of irreversibilities, as well as the limit for reversible operation. Despite these similarities, the new approach uses a general dimensionless model in which an effort is made to present the optimization results in terms of variables that are commonly available for actual engines. This includes the equivalent efficiency that accounts for irreversibilities for the compression and expansion components through the commonly available isentropic efficiencies, while most of the models use an irreversibility parameter that, although containing the same information, is rarely used in practical situations. In addition, we present the results in terms of an effective conductance ratio between heat exchangers (rM). This parameter compares the conductance of the heat exchangers and the characteristics of the fluids involved including specific heat capacity and mass flow rate.

2 Model

A schematic diagram of a heat engine operating between hot and cold thermal reservoirs is presented in Fig. 1. In addition to finite heat transfer rate between the engine and the two reservoirs, variable reservoir temperatures and isentropic efficiencies in the compression and expansion components are considered. The inclusion of variable reservoir temperatures adds a level of reality to the model because most heat engines are driven by streams at hot and cold heat exchangers whose temperature varies. In addition, this consideration allows the incorporation of the effects of hot and cold mass flow rates and thermophysical properties of the external streams. From the diagram, heat input at a rate Q_H is transferred to the high-pressure working fluid in a heat exchanger (heat input heat exchanger) increasing its temperature. The fluid is then expanded in the expansion component (turbine or piston–cylinder) to produce power (W_{tr}). A fraction of the energy gets dissipated as heat in this component due to irreversibilities (friction between piston and cylinder or turbine blades and the working fluid), which are accounted through the isentropic efficiency (η_t). This loss is transferred to the cold thermal reservoir at a rate of Q_{Lt}, see Fig. 1(*a*). After expansion, the fluid dissipates heat to the cold reservoir Q_{Lc} through a heat exchanger (heat dissipation heat exchanger) and then passes through the compression component (compressor, pump, or piston–cylinder) where its pressure increases. The isentropic compression efficiency considers the irreversibilities in this component. After compression, additional increase in the fluid temperature and entropy occurs with respect to the ideal process. This additional heat (Q_{LP}) remains in the fluid and is represented in Fig. 1(*a*) by the arrow pointing the engine's heat input Q_H. Finally, the high-pressure fluid enters the heat input heat exchanger, and the cycle is repeated. To simplify the model and analysis, irreversibilities in the compression device are merged with those for the expansion component, see Fig. 1(*b*). This diagram presents the reversible net power output (W_i) of the heat engine and the real net power output W_r that considers energy losses in the compression and expansion processes. In this case, the isentropic efficiencies are

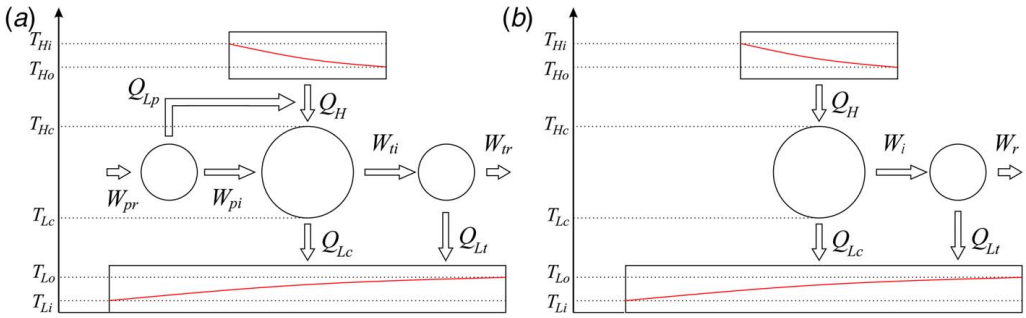

Fig. 1 Schematic diagram of the heat engine with variable reservoir temperatures and compression–expansion irreversibilities

lumped together into the isentropic equivalent efficiency (η_{eq}) defined in Sec. 2.1.

2.1 Isentropic Efficiencies. Based on the diagram presented in Fig. 1(*a*), the real and reversible net power output (W_r and W_i) for the heat engine can be, respectively, expressed as follows:

$$W_r = W_{rt} - W_{rp} = Q_H - Q_{Lc} - Q_{Lt} \tag{1}$$

$$W_i = W_{it} - W_{ip} = Q_H - Q_{Lc} \tag{2}$$

The isentropic compression and expansion efficiencies are defined by

$$\eta_p = \frac{W_{ip}}{W_{rp}} \tag{3}$$

$$\eta_t = \frac{W_{rt}}{W_{it}} \tag{4}$$

Similarly, the real and ideal net power outputs for the engine can be related with an isentropic equivalent efficiency η_{eq} that accounts for the losses in the compression and expansion components:

$$\eta_{eq} = \frac{W_r}{W_i} \tag{5}$$

Replacing Eqs. (2)–(5) into Eq. (1), the real power output yields:

$$W_r = \eta_{eq}\left(\frac{W_{rt}}{\eta_t} - \eta_p W_{rp}\right) \tag{6}$$

Defining the power ratio W_{rp}/W_{rt} as a parameter that accounts for the fraction of the produced power that is used to run the compression component and using Eqs. (1) and (6), the following expression for the η_{eq} can be obtained:

$$\eta_{eq} = \frac{\eta_t(1 - W_{rp}/W_{rt})}{1 - \eta_t\eta_p W_{rp}/W_{rt}} \tag{7}$$

The behavior of η_{eq} as a function of W_{rp}/W_{rt} is presented in Fig. 2, for different values of η_p and η_t. From Eq. (7) and Fig. 2, it is clear that if $W_{rp} = 0$ or $W_{rp} \ll W_{rt}$, then $W_{rp}/W_{rt} \cong 0$ and $\eta_{eq} \cong \eta_t$. This situation represents a heat engine where the power in the compression device is negligible with respect to the power produced in the turbine. This could describe the operation of some cycles using a pump to increase the pressure in the fluid; consequently, in this type of cycles, the isentropic efficiency for the turbine has a higher impact on η_{eq}; if $W_{rp} = W_{rt}$, then $W_{rp}/W_{rt} = 1$ and $\eta_{eq} = 0$. For this case, the compression device consumes all the power produced in the turbine and the cycle is "zero" efficient. In real engines $0 < W_{rp}/W_{rt} < 1$, and in particular for a Rankine cycle, W_{rp} could represent around 5% of W_{rt}. In Brayton cycles, for instance, W_{rp} could represent more than 40% of W_{rt}. From Fig. 2, for lower values of W_{rp}/W_{rt}, η_t exerts a strong impact in η_{eq} and defines the initial value for the curves. As expected, the effect of η_p is small for low W_{rp}/W_{rt} and its impact on η_{eq} becomes stronger as W_{rp}/W_{rt} increases. For a cycle characterized by a value of $W_{rp}/W_{rt} \approx 0.05$, η_{eq} is practically independent on η_p and proportional to η_t. In turn, for a cycle having a $W_{rp}/W_{rt} \approx 0.4$, η_{eq} could be as low as 0.65 for $\eta_p = \eta_t = 0.8$. It is worth noting that η_{eq} incorporates a combined effect of η_t and η_p. For instance, η_{eq} resulting from equal values for η_t and η_p (different than 1.0) is lower than such common value. In addition, as the role of the compression is magnified by increasing W_{rp}/W_{rt}, this combined effect increases, leading to a reduced η_{eq}. From Fig. 2, the range for η_{eq} goes from around 0.6 to 1.0, which covers the most common types of heat engines like Brayton ($\eta_{eq} = 0.65$–0.8), Rankine and Organic Rankine cycles ($\eta_{eq} = 0.8$–0.9), and internal combustion engines $\eta_{eq} = 0.6$–0.8. Then, the results are presented in terms of three values of η_{eq} (1.0, 0.8, and 0.6) that are representative of this range.

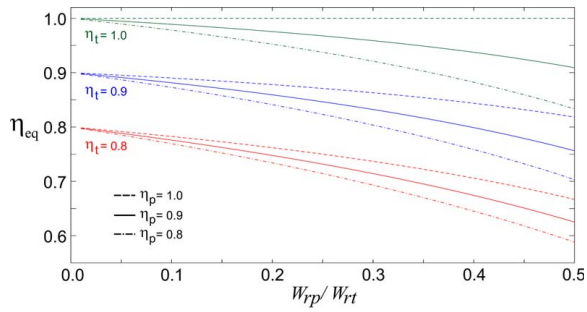

Fig. 2 Isentropic equivalent efficiency versus power ratio for different η_t and η_p values

2.2 Engine Model. The heat transfer rate between the hot/cold reservoirs and the reversible compartment can be, respectively, expressed in terms of the logarithmic mean temperature difference as follows:

$$Q_H = (UA)_H T_{Hi} \frac{(1 - \tau_H) - (D_H - \tau_H)}{\ln((1 - \tau_H)/(D_H - \tau_H))} = (\dot{m}c_p)_H T_{Hi}(1 - D_H) \tag{8}$$

$$Q_L = (UA)_L T_{Li} \frac{(1/\tau_L - 1) - (1/\tau_L - 1/D_L)}{\ln((1/\tau_L - 1)/(1/\tau_L - 1/D_L))} = (\dot{m}c_p)_L T_{Li}(1/D_L - 1) \tag{9}$$

where $\tau_H = T_{Hc}/T_{Hi}$, $\tau_L = T_{Li}/T_{Lc}$, $D_H = T_{Ho}/T_{Hi}$, and $D_L = T_{Li}/T_{Lo}$.

From the right side of Eqs. (8) and (9),

$$\ln\left(\frac{1-\tau_H}{D_H-\tau_H}\right)=\frac{(UA)_H}{(\dot{m}c_p)_H}\Rightarrow\frac{1-\tau_H}{D_H-\tau_H}=e^{\mathrm{NTU}_H} \tag{10}$$

$$\ln\left(\frac{1/\tau_L-1}{1/\tau_L-1/D_L}\right)=\frac{(UA)_L}{(\dot{m}c_p)_L}\Rightarrow\frac{1/\tau_L-1}{1/\tau_L-1/D_L}=e^{\mathrm{NTU}_L} \tag{11}$$

with $\mathrm{NTU}_H=(UA)_H/(\dot{m}c_p)_H$ and $\mathrm{NTU}_L=(UA)_L/(\dot{m}c_p)_L$ being, respectively, the number of transfer units for the heat input and heat dissipation heat exchangers.

Replacing Eqs. (10) and (11) into the left side of Eqs. (8) and (9), respectively, the heat input and total heat rejection rates (including the engine heat rejection and the heat loss) yield:

$$Q_H=(UA)_H T_{Hi}\frac{(1-e^{-\mathrm{NTU}_H})}{\mathrm{NTU}_H}(1-\tau_H) \tag{12}$$

$$Q_L=Q_{Lc}+Q_{Li}=(UA)_L T_{Li}\frac{(1-e^{-\mathrm{NTU}_L})}{\mathrm{NTU}_L}(1/\tau_L-1) \tag{13}$$

The following expression for the heat loss (Q_{Li}) is obtained from Eqs. (1), (2), and (5):

$$Q_{Li}=(1-\eta_{\mathrm{eq}})(Q_H-Q_{Lc}) \tag{14}$$

In turn, the engine heat rejection rate (Q_{Lc}) can be found from Eqs. (12)–(14):

$$Q_{Lc}=(UA)_L T_{Li}\frac{1}{\eta_{\mathrm{eq}}}\frac{(1-e^{-\mathrm{NTU}_L})}{\mathrm{NTU}_L}(1/\tau_L-1)-(UA)_H T_{Hi}\frac{(1-e^{-\mathrm{NTU}_H})}{\mathrm{NTU}_H}(1-\tau_H)\frac{(1-\eta_{\mathrm{eq}})}{\eta_{\mathrm{eq}}} \tag{15}$$

The operation of the heat engine is constrained to the reversible operation of the Carnot engine, for which the entropy balance yields:

$$\frac{Q_H}{T_{Hc}}=\frac{Q_{Lc}}{T_{Lc}} \tag{16}$$

Replacing Eqs. (8) and (15) into Eq. (16) and using the expressions of Eqs. (10) and (11) result in the following equation that relates τ_H, τ_L, and τ:

$$\left(\frac{1}{\tau_H}-1\right)=\frac{rM}{\eta_{\mathrm{eq}}}\left(1-\frac{1}{\tau_L}\right)-\frac{1}{\tau}\frac{1}{\tau_L}(1-\tau_H)\frac{(1-\eta_{\mathrm{eq}})}{\eta_{\mathrm{eq}}} \tag{17}$$

In Eq. (17), τ corresponds to the cold and hot input reservoir temperature ratio ($\tau=T_{Li}/T_{Hi}$), $M=(1-e^{-\mathrm{NTU}_L})\mathrm{NTU}_H/(1-e^{-\mathrm{NTU}_H})\mathrm{NTU}_L$, and $r=(UA)_L/(UA)_H$ are parameters that, respectively, represent design and operating characteristics (M) and the ratio between conductances (r) of heat input and heat dissipation heat exchangers. Both parameters can be lumped together into a single parameter $rM=[(\dot{m}c_p)_L(1-e^{-\mathrm{NTU}_L})]/[(\dot{m}c_p)_H(1-e^{-\mathrm{NTU}_H})]$, which can be seen as an effective conductance ratio between heat exchangers that compares the conductance and fluid characteristics including specific heat capacity and mass flow rate.

Solving for τ_L, Eq. (17) yields:

$$\tau_L=\frac{rM-(\eta_{\mathrm{eq}}/\tau_H)(1-\tau_H)}{rM+((1-\eta_{\mathrm{eq}})/\tau)(1-\tau_H)} \tag{18}$$

From Eqs. (2) and (5),

$$W_r=\eta_{\mathrm{eq}}(Q_H-Q_{Lc}) \tag{19}$$

Replacing the values of Q_H, Q_{LC} (Eqs. (12) and (15)), and τ_L (Eq. (18)) into Eq. (19), the power output for the real heat engine becomes

$$W_r=(UA)_H T_{Hi}\frac{(1-e^{-\mathrm{NTU}_H})}{\mathrm{NTU}_H}\frac{\eta_{\mathrm{eq}}(1-\tau_H)[rM\tau_H+\tau_H-rM\tau-1]}{\tau_H(rM+\eta_{\mathrm{eq}})-\eta_{\mathrm{eq}}} \tag{20}$$

Defining the non-dimensionalization factor $Q_{\max}$ as the maximum possible heat transfer rate between the hot and cold reservoirs (when no heat engine is present):

$$Q_{\max}=\frac{1}{4}(UA)_s T_{Hi}(1-\tau)\frac{\varepsilon_s}{\mathrm{NTU}_s} \tag{21}$$

where $\varepsilon_s(UA)_s/\mathrm{NTU}_s=\varepsilon_H(UA)_H/\mathrm{NTU}_H+(UA)_L\varepsilon_L/\mathrm{NTU}_L=(1+rM)\varepsilon_H(UA)_H/\mathrm{NTU}_H$ accounts for the total effective conductance in both heat exchangers, being $\varepsilon_L=1-e^{-\mathrm{NTU}_L}$ and $\varepsilon_H=1-e^{-\mathrm{NTU}_H}$.

Normalizing the power output (Eq. (20)) and the heat input (Eq. (12)) using the definition of $Q_{\max}$, expressions for dimensionless power output (W^*) and dimensionless heat input (Q_H^*) are obtained:

$$W^*=4\frac{\eta_{\mathrm{eq}}(1-\tau_H)[rM\tau_H+\tau_H-rM\tau-1]}{(1-\tau)(1+rM)[\tau_H(rM+\eta_{\mathrm{eq}})-\eta_{\mathrm{eq}}]} \tag{22}$$

$$Q_H^*=\frac{4(1-\tau_H)}{(1-\tau)(1+rM)} \tag{23}$$

Finally, from Eqs. (22) and (23), the heat engine efficiency can be found as

$$\eta=\frac{W^*}{Q_H^*}=\frac{\eta_{\mathrm{eq}}[rM\tau_H+\tau_H-rM\tau-1]}{\tau_H(rM+\eta_{\mathrm{eq}})-\eta_{\mathrm{eq}}} \tag{24}$$

2.3 Efficiency at Maximum Power Output. The maximum power output ($W^*_{\max}$) can be found by maximizing W^* with respect to τ_H, i.e., $dW^*/d\tau_H=0$:

$$W^*_{\max}=\frac{4rM\eta_{\mathrm{eq}}}{(rM+\eta_{\mathrm{eq}})^2}\frac{\left(\sqrt{\eta_{\mathrm{eq}}(\tau-1)+(rM\tau+1)}-\sqrt{rM+1}\right)^2}{(rM+1)(1-\tau)} \tag{25}$$

with the corresponding $\tau_{H,\mathrm{opt}}$ determined as

$$\tau_{H,\mathrm{opt}}=\frac{\eta_{\mathrm{eq}}+(rM/(rM+1))\sqrt{(rM+1)[\eta_{\mathrm{eq}}(\tau-1)+(rM\tau+1)]}}{rM+\eta_{\mathrm{eq}}} \tag{26}$$

Defining τ_c as the cold to hot thermal engine temperature ratio ($\tau_c=T_{Lc}/T_{Hc}$) and using the definition of τ, τ_L, and τ_H, $\tau_c=\tau/(\tau_L\tau_H)$. After replacing $\tau_{H,\mathrm{opt}}$ in this last equation, the corresponding $\tau_{c,\mathrm{opt}}$ is determined as

$$\tau_{c,\mathrm{opt}}=\frac{\sqrt{(rM+1)[\eta_{\mathrm{eq}}(\tau-1)+(rM\tau+1)]}-(1-\eta_{\mathrm{eq}})}{(rM+\eta_{\mathrm{eq}})} \tag{27}$$

Finally, from the expression for $W^*_{\max}$ (Eq. (25)), the efficiency at maximum power output ($\eta_{@\,W_{\max}}$) can be found as follows:

$$\eta_{@\,W^*_{\max}}=\frac{W^*_{\max}}{Q_H^*}=\eta_{\mathrm{eq}}\frac{(rM+1)}{(rM+\eta_{\mathrm{eq}})}\left[1-\sqrt{\frac{\eta_{\mathrm{eq}}(\tau-1)+(rM\tau+1)}{(rM+1)}}\right] \tag{28}$$

It can be easily verified that the Curzon–Ahlborn efficiency $\left(\eta_{@\,W_{max}}=1-\sqrt{\tau}\right)$ can be retrieved for a reversible engine with constant reservoir temperatures and ideal operation of compression and expansion components, i.e., $\eta_{\mathrm{eq}}=1$ and $rM=1$.

Equations (25)–(28) are general expressions for $W^*_{\max}$, $\tau_{H,\mathrm{opt}}$, $\tau_{c,\mathrm{opt}}$, and $\eta_{@\,W^*_{\max}}$, respectively. These expressions incorporate the

Table 1 Expressions for $\tau_{c,opt}$, W^*_{max}, and $\eta_{@\,W^*_{max}}$ considering different model characteristics

Model	Expressions for $\tau_{c,opt}$, W^*_{max}, and $\eta_{@\,W^*_{max}}$
Heat engine with constant heating and cooling flow temperatures 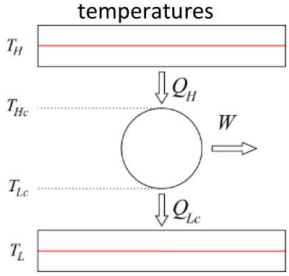	$\tau_{c,opt} = \sqrt{\tau}$ $W^*_{max} = \left(\frac{r}{r+1}\right)\left(1-\sqrt{\tau}\right)^2$ $\eta_{@\,W^*_{max}} = 1-\sqrt{\tau}$
Heat engine with variable heating and cooling flow temperatures 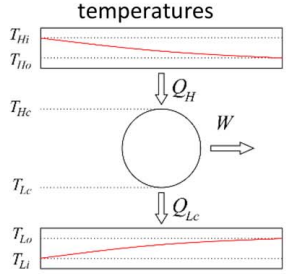	$\tau_{c,opt} = \sqrt{\tau}$ $W^*_{max} = \left(\frac{rM}{rM+1}\right)\left(1-\sqrt{\tau}\right)^2$ $\eta_{@\,W^*_{max}} = 1-\sqrt{\tau}$
Heat engine with constant heating and cooling temperatures and irreversibilities in compression and expansion components 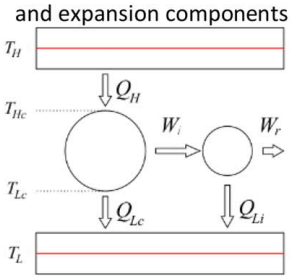	$\tau_{c,opt} = \frac{\sqrt{(r+1)\left[\eta_{eq}(\tau-1)+(r\tau+1)\right]}-(1-\eta_{eq})}{(r+\eta_{eq})}$ $W^*_{max} = \frac{4r\eta_{eq}}{(r+\eta_{eq})^2}\frac{\left(\sqrt{\eta_{eq}(\tau-1)+(r\tau+1)}-\sqrt{r+1}\right)^2}{(r+1)(1-\tau)}$ $\eta_{@\,W^*_{max}} = \eta_{eq}\frac{(r+1)}{(r+\eta_{eq})}\left[1-\sqrt{\frac{\eta_{eq}(\tau-1)+(r\tau+1)}{(r+1)}}\right]$
Heat engine with variable heating and cooling temperatures and irreversibilities in compression and expansion components 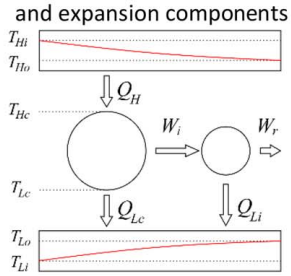	$\tau_{c,opt} = \frac{\sqrt{(rM+1)\left[\eta_{eq}(\tau-1)+(rM\tau+1)\right]}-(1-\eta_{eq})}{(rM+\eta_{eq})}$ $W^*_{max} = \frac{4rM\eta_{eq}}{(rM+\eta_{eq})^2}\frac{\left(\sqrt{\eta_{eq}(\tau-1)+(rM\tau+1)}-\sqrt{rM+1}\right)^2}{(rM+1)(1-\tau)}$ $\eta_{@\,W^*_{max}} = \eta_{eq}\frac{(rM+1)}{(rM+\eta_{eq})}\left[1-\sqrt{\frac{\eta_{eq}(\tau-1)+(rM\tau+1)}{(rM+1)}}\right]$

effect of variable heating and cooling flow temperatures and isentropic efficiencies at compression and expansion components. A summary of these expressions is presented in Table 1 for the heat engine considering constant and variable heating and cooling flow temperatures, and also with and without compression–expansion irreversibilities.

3 Results and Analysis

In this section, results from the model presented in Sec. 2 are illustrated for different values of heat engine parameters τ, rM, and η_{eq}. As explained before, there is an optimal value of τ_c (Eq. (27)) at which the power output achieves a maximum value

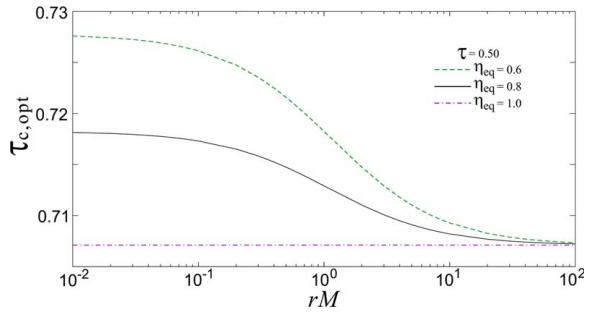

Fig. 4 $\tau_{c,opt}$ **as a function of** rM **for** $\tau = 0.5$, $\eta_{eq} = 1.0$, 0.8, **and 0.6**

(Eq. (25)). Figure 3 presents the behavior of $\tau_{c,opt}$ as a function of τ for three selected values of $\eta_{eq} = 0.6$, 0.8, and 1.0 and five values with different order of magnitude for rM. From this figure, higher τ values (lower difference between cold and hot reservoir temperatures) lead to higher $\tau_{c,opt}$. For the ideal case where $\eta_{eq} = 1.0$, when τ approaches 1.0, $\tau_{c,opt}$ also approaches 1.0, see Fig. 3(*a*), which implies a reduction in the temperature difference (potential) between reservoirs, and consequently a decrement in the power output. In the limit, when $\tau = \tau_{c,opt} = 1$, W and η are equal to zero. It is important to note that $\tau_{c,opt}$ is independent of the parameter rM for $\eta_{eq} = 1.0$. For values of $\eta_{eq} = 0.8$ (Fig. 3(*b*)) and $\eta_{eq} = 0.6$ (Fig. 3(*c*)), $\tau_{c,opt}$ is slightly higher for lower values of τ, when compared with the ideal scenario of Fig. 3(*a*); this means that for the same τ and $\eta_{eq} < 1.0$, irreversibilities in compression and expansion processes reduce the difference between cold and hot engine temperatures decreasing its power and efficiency. As expected, the larger the irreversibilities (smaller values of η_{eq}), the higher $\tau_{c,opt}$ for any value of $\tau < 1.0$, as can be seen in Figs. 3(*b*) and 3(*c*). From these figures, it can be appreciated that the parameter rM becomes important as the irreversibilities in the compression and expansion processes increase. This effect is more significant for lower τ values, i.e., for heat engines, such as Brayton engines, that operate with a larger difference between cold and hot reservoir temperatures, when compared with engines whose operation is framed by higher τ like organic Rankine cycles. Higher values of rM tend to reduce $\tau_{c,opt}$ for the same η_{eq}, which means that a larger effective conductance in the cold dissipation heat exchanger should help compensate the detriment in engine's performance due to irreversibilities.

In order to better appreciate the effect of rM on $\tau_{c,opt}$, Fig. 4 displays curves of $\tau_{c,opt}$ for five orders of magnitude values of rM, considering three η_{eq} and $\tau = 0.5$. For $\eta_{eq} = 1.0$, $\tau_{c,opt} = 0.707$, and, as it was mentioned, it is independent of rM. As η_{eq} reduces, $\tau_{c,opt}$ increases along the entire rM range; however, $\tau_{c,opt}$ reduces as rM increases, approaching to the corresponding value of $\tau_{c,opt}$ when $\eta_{eq} = 1.0$, in this case 0.707. It is worth noting that for $\tau = 0.5$, the maximum change in $\tau_{c,opt}$ in the analyzed rM range is about 0.02 (from $\tau_{c,opt} = 0.707$ for $\eta_{eq} = 1.0$ to $\tau_{c,opt} = 0.728$ for $\eta_{eq} = 0.6$), but this change is greater for lower τ values and, in the limit when $\tau \to 0.0$, $\tau_{c,opt}$ approaches this maximum change of about 0.386 (from $\tau_{c,opt} = 0.0$ for $\eta_{eq} = 1.0$ to $\tau_{c,opt} = 0.386$ for $\eta_{eq} = 0.6$), as can be seen in Fig. 3.

Figure 5 shows how W^*_{max} changes with τ for different orders of magnitude in the value of rM (from 10^{-2} to 10^{2}) and three different values of η_{eq} 0.6, 0.8, and 1. In general terms, W^*_{max} decreases with τ as expected, which is a result of smaller temperature differences between the heat source and the heat sink. In the extreme case $\tau = 1$, when both heat source and sink have the same temperature, W^*_{max} is naturally equal to zero for all situations, as the power generation's driving effect for the engine vanishes.

The largest possible value of $W^*_{max} = 1$ occurs when $\eta_{eq} = 1$, $rM = 1$, and $\tau = 0$ (equivalent to $T_L = 0$ or $T_H = \infty$). In this case W^*_{max} becomes equal to the heat transfer between the reservoirs when no heat engine is present. In any other situation, W^*_{max} is a fraction of such bound on the amount of energy that could be transferred between heat source and heat sink, which is due to a reduction in the heat-to-power conversion efficiency when τ increases (closer T_L and T_H), a decrease in η_{eq}, or because the balance in heat exchanger inventory between hot and cold sides is substantially altered.

As described in the model, rM represents an effective conductance ratio between heat input and heat dissipation heat exchangers. Figure 5 shows how taking rM away from 1 (order of magnitude 10^0) brings down W^*_{max}. As can be verified, for rM equal to 10^{-1} or 10^1, W^*_{max} is reduced in more than 50% for any value of τ and η_{eq}. For rM equal to 10^{-2} or 10^2, W^*_{max} reduction is even greater. In order to better capture this behavior, Figs. 6(*a*) and 6(*b*) present W^*_{max} as a function of rM for constant values of τ and η_{eq}. As can be seen, there is always a maximum value of W^*_{max} for rM

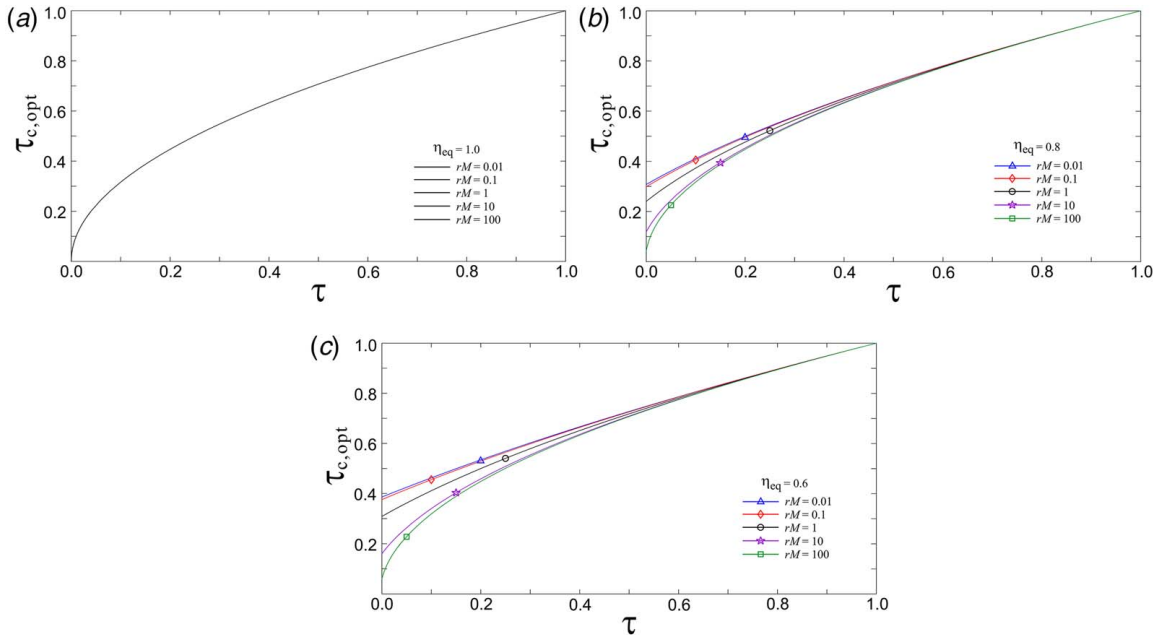

Fig. 3 $\tau_{c,opt}$ **as a function of** τ **for** $rM = 0.01$, 0.1, 1.0, 10, **and 100. (***a***)** $\eta_{eq} = 1.0$, **(***b***)** $\eta_{eq} = 0.8$, **and (c)** $\eta_{eq} = 0.6$.

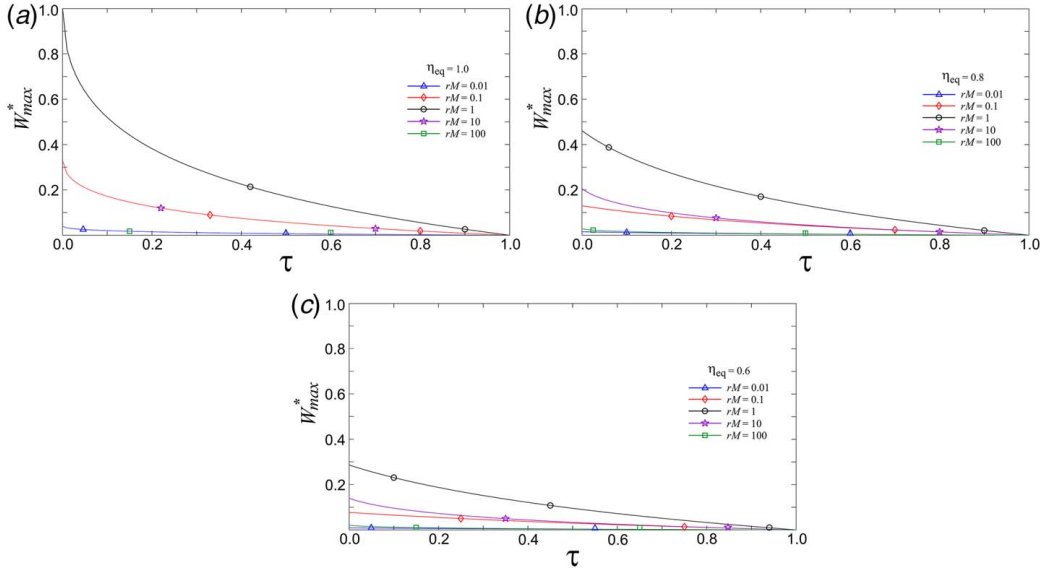

Fig. 5 W_{max} **as a function of** τ **for** $rM = 0.01, 0.1, 1, 10, 100$. **(*a*)** $\eta_{eq} = 1.0$, **(*b*)** $\eta_{eq} = 0.8$, **and (c)** $\eta_{eq} = 0.6$.

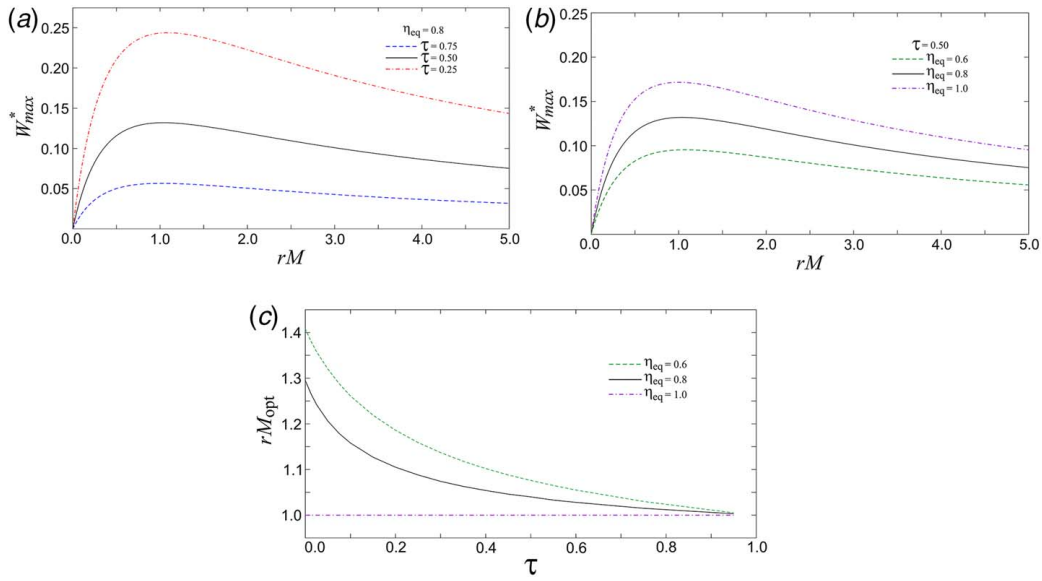

Fig. 6 **(*a*)** W^*_{max} **as a function of** rM **for** $\eta_{eq} = 0.8$ **and** $\tau = 0.25, 0.50, 0.75$. **(*b*)** W^*_{max} **as a function of** rM **for** $\tau = 0.5$ **and** $\eta_{eq} = 0.6, 0.8, 1.0$. **(*c*)** rM_{opt} **as a function of** τ **for** $\eta_{eq} = 0.6, 0.8, 1.0$

around 1. If the locus of maxima in Figs. 6(*a*) and 6(*b*) are isolated, the corresponding values of rM_{opt} as a function of τ and η_{eq} can be found, as shown in Fig. 6(*c*). Values of rM_{opt} are almost entirely between 1 and 1.2 for the considered values in this work. If τ or η_{eq} go very low (lower than approximately 0.2 and 0.6, respectively), rM_{opt} can start rising beyond 1.2 but in any case not much higher than 1.4. It is worth remembering that a value of rM higher than 1 means a larger heat exchanger (larger effective conductance) in the cold side when compared with the hot side. rM_{opt} becomes significant in practical implementations when a decision has to be made on the allocation of conductance of heat exchangers mainly driven by economic considerations.

Table 2 helps emphasizing the importance of heat exchangers' conductance allocation. Different values of W^*_{max} are presented as a function of rM and τ together with the percentual deviation with respect to the maximum possible W^*_{max} ($W^*_{max,max}$) for each case. As can be seen, choosing rM equal to 1.0 produces a W^*_{max} close to the optimum for all cases considered. If one of the heat

Table 2 Effect of optimizing heat exchanger conductance allocation, $\eta_{eq} = 0.8$

τ	rM	W^*_{max}	$\frac{W^*_{max,max} - W^*_{max}}{W^*_{max,max}}$ (%)
0.25	0.5	0.21054	13.65
	1	0.24339	0.18
	$rM_{opt} = 1.088$	$W^*_{max,max} = 0.24382$	–
	2	0.22265	8.68
0.50	0.5	0.11573	12.27
	1	0.13187	0.04
	$rM_{opt} = 1.040$	$W^*_{max,max} = 0.13192$	–
	2	0.11876	9.98
0.75	0.5	0.05003	11.56
	1	0.05657	6.02×10^{-3}
	$rM_{opt} = 1.015$	$W^*_{max,max} = 0.05657$	–
	2	0.05054	10.67

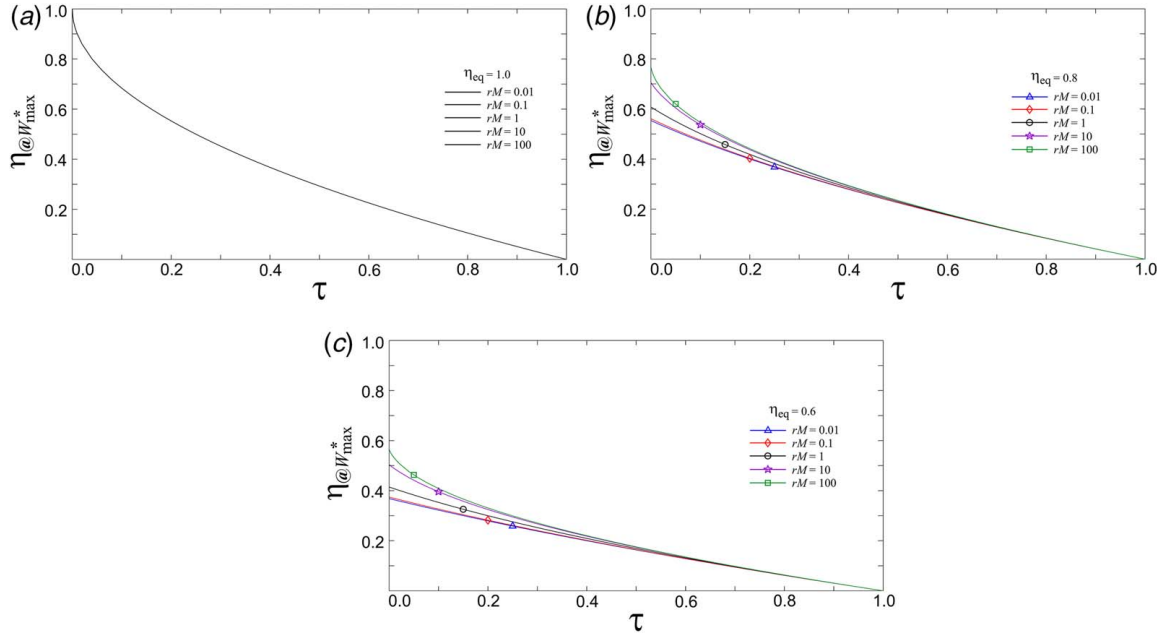

Fig. 7 $\eta_{@\ W^*_{max}}$ **as a function of** τ **for** $rM = 0.01, 0.1, 1, 10, 100$. **(*a*)** $\eta_{eq} = 1.0$, **(*b*)** $\eta_{eq} = 0.8$, **and (*c*)** $\eta_{eq} = 0.6$.

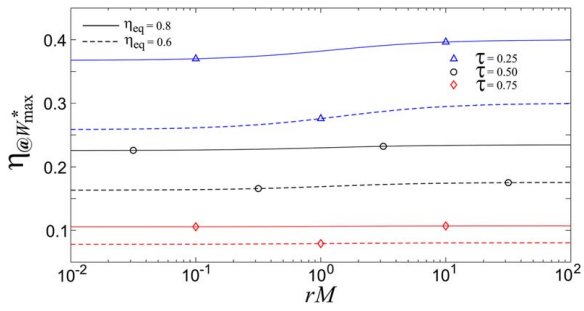

Fig. 8 $\eta_{@\ W^*_{max}}$ **as a function of** rM **for** $\tau = 0.25, 0.50, 0.75$ **and** $\eta_{eq} = 0.8$ **and 0.6**

exchangers is twice large than the other, the percentual deviation respect to $W^*_{max,\,max}$ is around 10%. These relative deviations are more significant for lower values of τ.

Figure 7 illustrates the effects of η_{eq} and rM on the dependence of the efficiency at maximum power as a function of the temperature ratio τ. When $\tau = 1$, the temperature gradient that drives the engine disappears, and at that point, independently of η_{eq} and rM, W^*_{max} goes to zero. This is also true for the Carnot efficiency. W^*_{max} increases monotonically as τ decreases and peaks in the limit $\tau \to 0$ when the low temperature reservoir tends to a temperature of absolute zero or the high temperature grows to infinity. Notice that differently from what occurred with the maximum power (see Fig. 5), in the case of $\eta_{eq} = 1$, the value of the rM has no effect on $\eta_{@\ W^*_{max}}$ (thus all curves collapse into one in Fig. 7(*a*)). As the compression or the expansion component efficiencies decrease, or the compressing power becomes more important with respect to the expansion power, η_{eq} decreases and so does $\eta_{@\ W^*_{max}}$. When $\eta_{eq} < 1$, the efficiency at maximum power drops as rM decreases.

Figure 8 reemphasizes the impact of the heat exchangers effective conductance ratio. In the range considered, which spans five orders of magnitude, it can be observed that for large τ, the efficiency at maximum power is essentially insensitive to the allocation of heat exchanger conductance and effectiveness represented by rM. When it does impact ($\tau < 0.5$) the behavior is essentially a smooth transition between a low limit value for $rM \ll 1$ and a higher value for $rM \gg 1$, with the inflection occurring near the point when the heat exchangers have equal allocation of effective conductance ($rM \sim 1$). Observe in Fig. 8 a trend that is common in heat engines; the impact of the cold heat exchanger is greater than the hot one in terms of efficiency. For example, in a Rankine cycle, a small variation in the condenser temperature has a larger impact on efficiency than the same variation in the boiler [7]. It can also be seen that the effect of rM on efficiency is not as high as it is for W^*_{max} (see Figs. 5 and 6). The meaning of a very large rM is allocating most of the available area to the cold heat exchanger, which implies $T_{LC} \to T_{Li}$ (see Fig. 1). After some point T_{LC} is so close to T_{Li} that any additional area allocated to the cold heat exchanger no longer increase the heat engine efficiency (the curve levels off for large values of rM). Similar situation occurs in the lower end value where most of the area is allocated to the hot heat exchanger and $T_{HC} \to T_{Hi}$.

4 Conclusions

A thermodynamic model considering finite heat transfer rate, variable heat source and sink temperature, and irreversibilities associated with the compression–expansion processes was developed to analyze the performance of heat engines operating under different thermodynamic cycles. Expressions for the optimum ratio between cold and hot thermal engine temperatures ($\tau_{c,opt}$), maximum power (W^*_{max}), and efficiency at maximum power output ($\eta_{@\ W^*_{max}}$) are obtained as a function of the parameters τ (cold and hot reservoirs temperature ratio), rM (effective conductance ratio between heat input and heat dissipation heat exchangers), and η_{eq} (equivalent isentropic efficiency). In all cases, the Curzon–Ahlborn efficiency is retrieved for $rM = 1.0$ and $\eta_{eq} = 1.0$. It was found that rM has no effect on $\tau_{c,opt}$, W^*_{max}, and $\eta_{@\ W^*_{max}}$ when $\eta_{eq} = 1.0$. As the isentropic efficiencies in the compression or the expansion components decrease, as a consequence of irreversibilities, η_{eq} decreases leading to reductions in W^*_{max}, $\eta_{@W_{max}}$, and in the difference between cold and hot engine temperatures (increment in $\tau_{c,opt}$). When $\eta_{eq} < 1$, $\tau_{c,opt}$ decreases and $\eta_{@\ W^*_{max}}$ increases with rM, respectively. In turn, W^*_{max} drops for rM away from 1.0 in more than one order of magnitude. Optimum rM values (rM_{opt}) leading to maximum power output are found to be between 1 and 1.4 for the analyzed ranges of τ and η_{eq}. rM_{opt} shifts to the upper limit of that range as irreversibilities increase (η_{eq} reduces) and/or for engines operating within higher temperature difference between cold and hot reservoirs (lower τ). In this case, the compression power is usually a significant portion of the net

power. A value of rM_{opt} slightly greater than 1.0 means that in order to achieve maximum power, the heat dissipation heat exchanger must be larger when compared with the heat exchanger at the hot side.

Acknowledgment

This research was primarily supported by the Mechanical and Thermal Engineering Sciences Center at National Renewable Energy Laboratory as a part of the Laboratory Directed Research and Development (LDRD) Program funded by the U.S. Department of Energy (DOE).

The views expressed in the article do not necessarily represent the views of the DOE or the U.S. Government.

Obie I. Abakporo acknowledges the support of the Florida A&M University Title III Fellowship and the facility usage of Florida State University Center of Advanced Power Systems.

Conflict of Interest

There are no conflicts of interest.

Data Availability Statement

The datasets generated and supporting the findings of this article can be obtained from the corresponding author upon reasonable request. The authors attest that all data for this study are included in the paper. Data provided by a third party are listed in Acknowledgment.

Nomenclature

A = effective heat transfer area, m^2
U = overall heat transfer coefficient, kW m^{-2} K^{-1}
$\dot{m}$ = mass flow rate, kg/s
c_p = specific heat at constant pressure, kJ kg^{-1} K^{-1}
D_H = T_{Ho} to T_{Hi} temperature ratio
D_L = T_{Li} to T_{Lo} temperature ratio
Q_H = heat input, kW
Q_{Lc} = heat rejection, kW
Q_{Lt} = heat loss, kW
Q_L = total heat rejection, kW
T_{Hi} = inlet hot reservoir temperature, K
T_{Li} = inlet cold reservoir temperature, K
T_{Hc} = hot heat engine temperature, K
T_{Lc} = cold heat engine temperature, K
T_{Ho} = exit hot reservoir temperature, K
T_{Lo} = exit cold reservoir temperature, K
W_r = net power output, kW
W_{rt} = expansion power, kW
W_{rp} = compression power, kW
W_i = reversible net power output, kW
W_{it} = reversible expansion power, W
W_{ip} = reversible compression power, kW
W^* = dimensionless power output
Q_H^* = dimensionless heat input rate
rM = effective conductance ratio between cold and hot side heat exchangers
NTU = number of transfer units
ε = effectiveness
η = thermal efficiency
$\eta_{@\ W^*_{max}}$ = efficiency at maximum power
η_t = isentropic efficiency expansion component
η_p = isentropic efficiency compression component
η_{eq} = equivalent isentropic efficiency
τ = cold to hot reservoirs temperature ratio
τ_c = cold to hot thermal engine temperature ratio
τ_H = T_{Hc} to T_{Hi} temperature ratio
τ_L = T_{Li} to T_{Lc} temperature ratio

Subscripts

H = high temperature
L = low temperature
max = maximum
opt = optimum

References

[1] Curzon, F. L., and Ahlborn, B., 1975, "Efficiency of a Carnot Engine at Maximum Power Output," Am. J. Phys., **43**(1), pp. 22–24.
[2] Chambadal, P., 1957, *Les Centrales Nucléaires*, Armand Colin, Paris.
[3] Novikov, I. I., 1958, "The Efficiency of Atomic Power Stations (a Review)," J. Nucl. Energy (1954), **7**(1–2), pp. 125–128.
[4] Esposito, M., Kawai, R., Lindenberg, K., and Van den Broeck, C., 2010, "Efficiency at Maximum Power of Low-Dissipation Carnot Engines," Phys. Rev. Lett., **105**(15), p. 150603.
[5] Huleihil, M., 2018, "Effective Temperature and Performance Characteristics of Heat Engines," Int. J. Thermodyn., **21**(3), pp. 128–134.
[6] Calvo-Hernández, A., Roco, J. M. M., Medina, A., Velasco, S., and Guzmán-Vargas, L., 2005, "The Maximum Power Efficiency $1-\sqrt{\tau}$: Research, Education, and Bibliometric Relevance," Eur. Phys. J., **224**(5), pp. 809–823.
[7] Bejan, A., 1998, *Advanced Engineering Thermodynamics*, Wiley, New York.
[8] Levario-Medina, S., Valencia-Ortega, G., and Arias-Hernandez, L. A., 2019, "Thermal Optimization of Curzon–Ahlborn Heat Engines Operating Under Some Generalized Efficient Power Regimes," Eur. Phys. J. Plus, **134**(7), p. 348.
[9] Iyyappan, I., and Johal, R. S., 2019, "Efficiency of a Two-Stage Heat Engine at Optimal Power," EPL, **128**(5), p. 50004.
[10] Chen, J., Yan, Z., Lin, G., and Andresen, B., 2001, "On the Curzon–Ahlborn Efficiency and Its Connection With the Efficiencies of Real Heat Engines," Energy Convers. Manage., **42**(2), pp. 173–181.
[11] Gutkowicz-Krusin, D., Procaccia, I., and Ross, J., 1978, "On the Efficiency of Rate Processes. Power and Efficiency of Heat Engines," J. Chem. Phys., **69**(9), p. 3898.
[12] Wu, C., and Kiang, R. L., 1992, "Finite-Time Thermodynamic Analysis of a Carnot Engine With Internal Irreversibility," Energy, **17**(12), pp. 1173–1178.
[13] Gordon, J. M., and Huleihil, M., 1992, "General Performance Characteristics of Real Heat Engines," J. Appl. Phys., **72**(3), pp. 829–837.
[14] Chen, J., 1998, "A Universal Model of an Irreversible Combined Carnot Cycle System and Its General Performance Characteristics," J. Phys. A: Math. Gen., **31**(15), pp. 3383–3394.
[15] Ikegami, Y., and Bejan, A., 1998, "On the Thermodynamic Optimization of Power Plants With Heat Transfer and Fluid Flow Irreversibilities," ASME J. Sol. Energy Eng., **120**(2), pp. 139–144.
[16] Bejan, A., 1996, "Maximum Power From Fluid Flow," Int. J. Heat Mass Transfer, **39**(6), pp. 1175–1181.
[17] Grazzini, G., 1991, "Work From Irreversible Heat Engines," Energy, **16**(4), pp. 747–755.
[18] Ibrahim, O. M., Klein, S. A., and Mitchell, J. W., 1991, "Optimum Heat Power Cycles for Specified Boundary Conditions," ASME J. Eng. Gas Turbines Power, **113**(4), pp. 514–521.
[19] Lee, W. Y., and Kim, S. S., 1991, "An Analytical Formula for the Estimation a Rankine Cycle Heat Engine Efficiency at Maximum Power," Int. J. Energy Res., **15**(3), pp. 149–159.
[20] Lee, W. Y., and Kim, S. S., 1991, "Power Optimization of an Irreversible Heat Engine," Energy, **16**(7), pp. 1051–1058.
[21] Singh, V., and Johal, R. S., 2018, "Low-Dissipation Carnot-Like Heat Engines at Maximum Efficient Power," Phys. Rev. E, **98**(6), p. 062132.
[22] Sahin, B., Kodal, A., and Yavuz, H., 1995, "Efficiency of a Joule-Brayton Engine at Maximum Power Density," J. Phys. D: Appl. Phys., **28**(7), pp. 1309–1313.
[23] Angulo-Brown, F., 1991, "An Ecological Optimization Criterion for Finite-Time Heat Engines," J. Appl. Phys., **69**(11), pp. 7465–7469.
[24] Durmayaz, A., Sogut, O. S., Sahin, B., and Yavuz, H., 2004, "Optimization of Thermal Systems Based on Finite-Time Thermodynamics and Thermoeconomics," Prog. Energy Combust. Sci., **30**(2), pp. 175–217.
[25] Ding, A., Chen, L., and Sun, F., 2011, "A Unified Description of Finite Time Exergoeconomic Performance for Seven Typical Irreversible Heat Engine Cycles," Int. J. Sustain. Energy, **30**(5), pp. 257–269.
[26] Bejan, A., 1991, *Entropy Generation Minimization: The Method of Thermodynamic Optimization of Finite-Size Systems and Finite-Time Processes*, CRC Press, Boca Raton, FL.
[27] Mironova, V. A., Tsirlin, A. M., Kazakov, V. A., and Berry, R. S., 1994, "Finite-Time Thermodynamics: Exergy and Optimization of Time-Constrained Processes," J. Appl. Phys., **76**(2), pp. 629–636.
[28] Tyagi, S. K., Kaushik, S. C., and Salhotra, R., 2002, "Ecological Optimization and Performance Study of Irreversible Stirling and Ericsson Heat-Engines," J. Phys. D: Appl. Phys., **35**(20), pp. 2668–2675.
[29] Chen, L., Zhou, J., Sun, F., and Wu, C., 2004, "Ecological Optimization for Generalized Irreversible Carnot-Engines," Appl. Energy, **77**(3), pp. 327–338.
[30] Arias-Hernández, L. A., Ares de Parga, G., and Angulo-Brown, F., 2004, "A Variational Ecological-Type Optimization of Some Thermal-Engine Models," Open Syst. Inf. Dyn., **11**(2), pp. 123–138.

[31] Ust, Y., Safa, A., and Sahin, B., 2005, "Ecological Performance Analysis of an Endoreversible Regenerative Brayton Heat Engine," Appl. Energy, **80**(3), pp. 247–260.
[32] Chen, L., Zhang, W., and Sun, F., 2007, "Power, Efficiency, Entropy Generation Rate and Ecological Optimization for a Class of Generalized Irreversible Universal Heat Engine Cycles," Appl. Energy, **84**(5), pp. 512–525.
[33] Calvo Hernández, A., Roco, J. M. M., Medina, A., and Sánchez-Salas, N., 2014, "Heat Engines and the Curzon–Ahlborn Efficiency," Rev. Mex. Fís., **60**(5), pp. 384–389.
[34] Van den Broeck, C., 2005, "Thermodynamic Efficiency at Maximum Power," Phys. Rev. Lett., **95**(19), p. 190602.
[35] Esposito, M., Lindenberg, K., and Van den Broeck, C., 2009, "Thermoelectric Efficiency at Maximum Power in a Quantum dot," EPL, **85**(6), p. 60010.